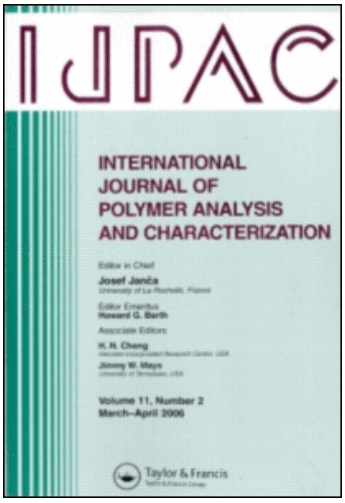

International Journal of Polymer Analysis and Characterization
Publication details, including instructions for authors and subscription information:
http://www.informaworld.com/smpp/title~content=t713646643

Polymer Films from Size Exclusion Chromatography Using A Solvent-Evaporation Interface: Analysis of Polymer Blends

P. C. Cheung[a]; S. Hsu[a]; M. Tempel[a]; S. T. Balke[a]; T. C. Schunk[b]; L. Li[b]; S. Sosnowski[c]; M. A. Winnik[c]
[a] Department of Chemical Engineering and Applied Chemistry, University of Toronto, Toronto, Canada [b] Analytical Technology Division, Eastman Kodak Company, Rochester, NY, USA [c] Department of Chemistry, University of Toronto, Toronto, Canada

To cite this Article Cheung, P. C. , Hsu, S. , Tempel, M. , Balke, S. T. , Schunk, T. C. , Li, L. , Sosnowski, S. and Winnik, M. A.(1996) 'Polymer Films from Size Exclusion Chromatography Using A Solvent-Evaporation Interface: Analysis of Polymer Blends', International Journal of Polymer Analysis and Characterization, 2: 3, 271 — 291
To link to this Article: DOI: 10.1080/10236669608233915
URL: http://dx.doi.org/10.1080/10236669608233915

Int. J. Polymer Analysis & Characterization
1996, Vol. 2, pp. 271–291
Reprints available directly from the publisher
Photocopying permitted by license only

Polymer Films from Size Exclusion Chromatography Using A Solvent-Evaporation Interface: Analysis of Polymer Blends

P.C. CHEUNG, S. HSU, M. TEMPEL and S.T. BALKE*

Department of Chemical Engineering and Applied Chemistry, University of Toronto, Toronto, Canada M5S 3E5

T.C. SCHUNK

Analytical Technology Division, Eastman Kodak Company, Rochester, NY, USA 14650-2136

L. LI, S. SOSNOWSKI and M.A. WINNIK

Department of Chemistry, University of Toronto, Toronto, Canada M5S 3H6

(Received October 17, 1994; in final form May 9, 1995)

Two solvent-evaporation interfaces were used for high-temperature and room-temperature size exclusion chromatography (SEC) to deposit fractions as dried polymer films on substrates. In the high-temperature SEC work, polymers of interest included polyethylene labeled with a fluorescent dye (4-nitrobenzo-2-oxa-1,3-diazole (NBD)), unlabeled polystyrene, unlabeled polypropylene, both individually and as blends of these polymers. Fourier-transform infrared (FTIR) spectroscopy, optical microscopy, laser confocal fluorescence microscopy, and fluorescence spectroscopy were used to analyze the films. FTIR spectroscopy results were readily affected by film morphologies. Resulting spectral inaccuracies included Christiansen distortion, wavy baselines, and changes in absorption band ratios. Laser confocal fluorescence microscopy results proved especially misleading with some labeled polyethylene failing to fluoresce. NBD-labeled poly(methyl methacrylate), unlabeled poly(methyl methacrylate), unlabeled polystyrene, NBD-labeled polystyrene, as well as blends of these polymers were analyzed using the room temperature SEC-evaporation interface system. No phase separation was observed in those blends. However, in an SEC run of phenanthrene-labeled polystyrene and anthracene-labeled poly(methyl methacrylate), steady-state fluorescence spectra did reveal the increasing diffuseness of the polymer-polymer interface as molecular size of the polymer blend components decreased.

KEY WORDS Polymer blends, solvent-evaporation interface, size exclusion chromatography, Fourier-transform infrared spectroscopy, laser confocal fluorescence microscopy, fluorescence spectroscopy

INTRODUCTION

Fractionation by size exclusion chromatography (SEC) followed by the use of one or more detectors that examine each fraction is one approach of attempting to obtain a comprehensive analysis of a polymer blend. There are limitations with both the fractionation and

*Presented at the 7th International Symposium of Polymer Analysis and Characterization, 1994.

detection aspects of this approach. A major source of detection limitations can be the presence of the mobile phase. For example, if mid-infrared detection is to be used by employing a conventional Fourier-transform infrared (FTIR) instrument with a flow-through cell, absorption of infrared light by the mobile phase means that only few wavelength "windows" are available where absorption by the polymer is measurable.

A solvent-evaporation interface removes the mobile phase and deposits each fraction as an isolated, dried polymer film on a germanium disc (or on some other substrate transparent to mid-infrared radiation). The series of deposited films are then analyzed using FTIR spectroscopy. Although there has been considerable work in the area of solvent-evaporation interface design for high performance liquid chromatography of small molecules, for SEC only two designs have emerged [1,2]. In assessments of these interfaces [3,4] concerns centered upon FTIR spectral fidelity, film quality, resolution and polymer recovery. The morphology of the deposited film proved to be a critical aspect with respect to the spectra obtained. Later work focused upon methods of obtaining acceptable morphologies [5] and examination of film morphology by optical microscopy is now a routine part of the analytical procedure in our laboratories.

In this paper, we show our most recent attempts to analyze polymer blends by using the solvent-evaporation interface-FTIR spectrometer combination. We also present results of a new attempt to expand the utility of the interface through the use of fluorescent-labeled polymers. This last-mentioned method involves the analysis of the deposited films by both laser confocal fluorescence microscopy and by fluorescence spectroscopy, in addition to FTIR spectroscopy and optical microscopy. In addition to providing a more in-depth understanding of the film morphology and how it relates to FTIR spectra, these newly applied techniques can be used to examine the degree to which one polymer is miscible in another as a function of molecular weight.

THEORY

FTIR Spectroscopy

FTIR spectroscopy has been used to measure the identity of polymer blend components, the quantity of each component (including additives), polymer microstructure (e.g., branching), intermolecular interactions, degree of crystallinity, and orientation. Therefore, it is potentially an extremely useful SEC detector, especially when used on dried polymer films where solvent absorption is not a factor. However, the fact that FTIR spectra can be used to determine such a multiplicity of properties also means that the spectra tend to be affected by more than one property.

Our earlier work has shown that the morphologies of the polymer films obtained from the interface can cause distortions in the spectra [5]. If the polymer film is not homogeneous and flat, scattering of the incoming infrared radiation may cause distortion in the spectra. The scattering can exhibit highly sloping baselines and may change the ratios of absorption bands in spectra. In the extreme case, Christiansen scattering causes highly distorted spectra with derivative-like absorption bands [6].

If the polymer film is discontinuous (i.e., bare spots or pinholes are present), then the measured absorbance under-represents the amount of polymer present. Figure 1 is a plot of measured absorbance ($A_{measured}$) against true absorbance (A_{true}) as a func-

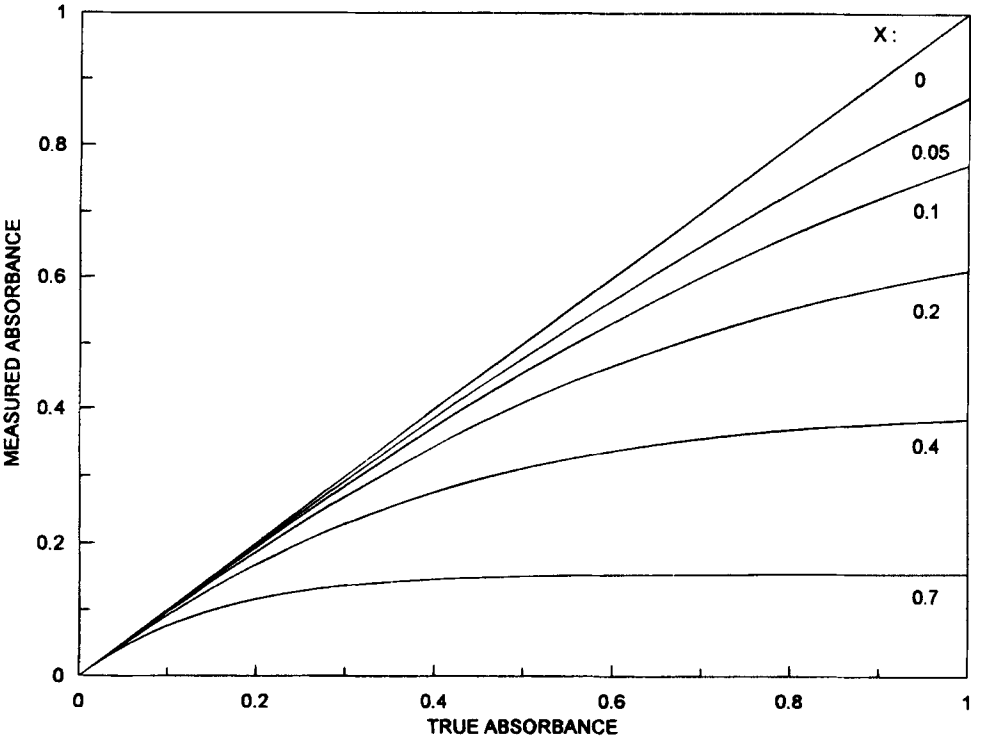

FIGURE 1 Deviation of measured absorbance ($A_{measured}$) form true absorbance (A_{true}) as a function of the fraction of bare surface (X) in sample according to Equation (1). (Reproduced with permission from reference 7. Copyright 1952 American Chemical Society).

tion of fraction of bare surface (X) on a sample. A_{true} is the absorbance of a continuous, uniform polymer film on a substrate and $A_{measured}$ is the measured absorbance of a discontinuous polymer film on a similar substrate. The total amount of polymer analyzed is identical for both films. The curves in Figure 1 were constructed using Beer's law with constant absorptivity from the following equation as first shown by Jones [7]:

$$A_{measured} = -\log((1 - X)\, 10^{\frac{A_{true}}{(X-1)}} + X) \quad (1)$$

Derivation of this equation assumes that both continuous and discontinuous films have constant (albeit different) thicknesses. The figure shows that the higher the absorbance of the band, the more sensitive it is to the effect of bare area. Furthermore, the effect of bare area is to cause the measured absorbance to become increasingly less than the true absorbance depending upon the value of X. This means that for a film with some bare area, inaccurate ratios of absorbances within the same spectrum can result to an extent dependent upon how different are the true absorbance values of the peaks: the greater the difference and the greater the fraction of bare area, the greater will be the inaccuracy in the measured absorbance ratio.

Laser Confocal Fluorescence Microscopy

The laser confocal fluorescence microscope (LCFM) is commonly used for fluorescent imaging. The two critically placed pinholes allows one to enhance the contrast in the region of interest by excluding all illumination light or out-of-focus fluorescent light [8]. Optical contrast between two polymers in a blend is achieved by labeling one polymer with a fluorescent dye. The fluorescent dye used here is 4-nitrobenzo-2-oxa-1,3-diazole (NBD) [9]. NBD has peak absorbance at 466 nm and peak emission at 520 nm. The laser used with the LCFM used emits light at 488 nm and the fluorescence detector is tuned to 520 nm. The laser/detector wavelengths correspond well to the absorbance/emission wavelengths of the dye, creating a high contrast between labeled and unlabeled polymers. This contrast allows direct examination of the morphology in the polymer blend.

Fluorescence Spectroscopy

Nonradiative energy transfer occurs in a system of two fluorescent species, where the emission spectrum of the first (donor) overlaps the excitation spectrum of the second (acceptor) so that excitation energy absorbed by the donor can be transferred to the acceptor at very small distances [10]. In a system of polymer blends where one is labeled with a donor and one with an acceptor, the energy transfer occurs at distances not exceeding 10 nm. Therefore, energy transfer can only occur at the interface between the two polymers in the blend. The measure of energy transfer, the ratio of the intensities of the donor to acceptor, I_D/I_A, is inversely proportional to the product of interface thickness and the surface area. The ratio can compensate for variations in the amount of polymer deposited in a given fraction from the solvent-evaporation interface. However, for this number to be a valid measure of energy transfer, it is assumed that the labels are randomly distributed throughout the polymer chains and fractions.

If these assumptions are valid, then by measuring energy transfer on the deposited films of each polymer blend fraction obtained from the solvent-evaporation interface, we obtain information with two important uses: (i) a quantitative characterization of interface morphology which we hope to eventually correlate with the accuracy of the resulting FTIR spectrum and, (ii) a measure reflecting both polymer blend dispersion (surface area) and miscibility (interface thickness) *as a function of molecular weight* for the pair of polymers. This latter type of information can be used to assist predictions of blend compatibility.

EXPERIMENT

Table I describes the experiments conducted in terms of samples injected and techniques used to analyze deposits on the disc. Experiments 1,2 and 3 were run in duplicate, others were run once only.

Materials

The NBD-labeled polyethylene was prepared from maleated linear low-density polyethylene at the University of Toronto. NBS 706 supplied by NIST (Washington, DC) was used as the unlabeled polystyrene in experiments 2 and 3. Unlabeled polypropylene used

TABLE I

SEC experimental protocol and techniques used to analyze deposits.

Experiment Number	Description	Microscopy		Spectroscopy	
		Optical	Laser Confocal Fluorescence	FTIR	Fluorescence
1	NBD-labeled polyethylene	X	X	X	
2	unlabeled polystyrene	X		X	
3	NBD-labeled polyethylene + unlabeled polystyrene	X	X	X	
4	NBD-labeled polyethylene + unlabeled polypropylene	X	X	X	
5	NBD-labeled poly(methyl methacrylate) + unlabeled poly(methyl methacrylate)	X	X	X	
6	NBD-labeled polystyrene + unlabeled poly(methyl methacrylate)	X	X	X	
7	NBD-labeled poly(methyl methacrylate) + unlabeled polystyrene	X	X	X	
8	Phenanthrene-labeled polystyrene + anthracene-labeled poly(methyl methacrylate)	X		X	X

was PP 180K supplied by American Polymer Standards (Mentor, Ohio). NBD- or anthracene (An)-labeled poly(methyl methacrylate) were prepared at the University of Toronto by two-stage emulsion polymerization. The fluorescent chromophore (NBD or An) and initiator were fed to a reactor containing a latex seed of methyl methacrylate. The molar ratio of chromophore to methyl methacrylate monomer is approximately 1:100 [11]. Polystyrene to be labeled with phenanthrene (Phe) was synthesized in a similar fashion. Unlabeled poly(methyl methacrylate) was prepared by emulsion polymerization at the University of Toronto. NBD-labeled polystyrene was prepared at the University of Toronto by using anionic polymerization with NBD attached to the end of the polystyrene chain during the polymerization. Unlabeled polystyrene used in experiment 7 was prepared by emulsion polymerization at the University of Toronto.

Size Exclusion Chromatography and Solvent-Evaporation Interface Design

For experiments 1 to 4 inclusive in Table I, a Waters 150C high-temperature size exclusion chromatograph (Milford, Massachusetts) equipped with a differential refractometer (DR) was used at a temperature of 145°C with 1,2,4-trichlorobenzene (TCB) as the mobile phase. The chromatograph was equipped with three PLgel (Polymer Laboratories, Amherst, Massachusetts) 10-μm mixed-bed analytical columns. Sample preparation involved dissolution of 0.2 wt % polymer sample (in a polymer blend, 0.15 wt % of each was used) in TCB with 0.2 wt % butylated hydroxytoluene as a stabilizer at 175°C for 2 h and 145°C for another 2 h before injection. Injection volume was 100 μL and flow rate was at 0.5 mL/min except for experiment 1 in which potassium chloride discs were used and the flow rate was set at 0.3 mL/min.

The solvent-evaporation interface design (denoted "Interface I") is based upon that developed by Dekmezian *et al.* [1]. Our modifications to this design were previously described [5]. For this work, additional modifications involved temperature monitoring. A schematic diagram of the device is shown in Figure 2. The thermocouples were placed close to the ring heater, close to the polymer solution spray, and inside the 120 kHz ultrasonic nozzle (model 8700-120MS from Sono-Tek, Poughkeepsie, New York). Since the vaporization of TCB absorbed latent heat, the thermocouples were used to monitor the temperature changes during the spray.

The vacuum oven was at 102–104°C and 8–13 kPa. The temperature at the heater surface was 200°C. Nozzle power was set at 0.5 W. Germanium discs (13-mm diameter and 1-mm thick) were used as substrates except for one trial of experiment 1 in which 2-mm thick potassium chloride discs with the same diameter were used. The potassium chloride discs were vapor coated with carbon by a Edwards Coating System E306A (Crawley, England) in order to provide better wetting characteristics. Polymer fractions of 1 min each were collected on each disc unless specified. The discs deposited with polymer films were then transferred from the solvent-evaporation interface to other analytical equipment for analysis as listed in Table I and described in the next section.

Polymer blend deposits of SEC fractions from samples corresponding to experiments 5 through 8 were prepared with a second interface design (denoted "Interface II"). SEC separations were performed at ambient temperature (24°C) with a Perkin Elmer Series 4 liq-

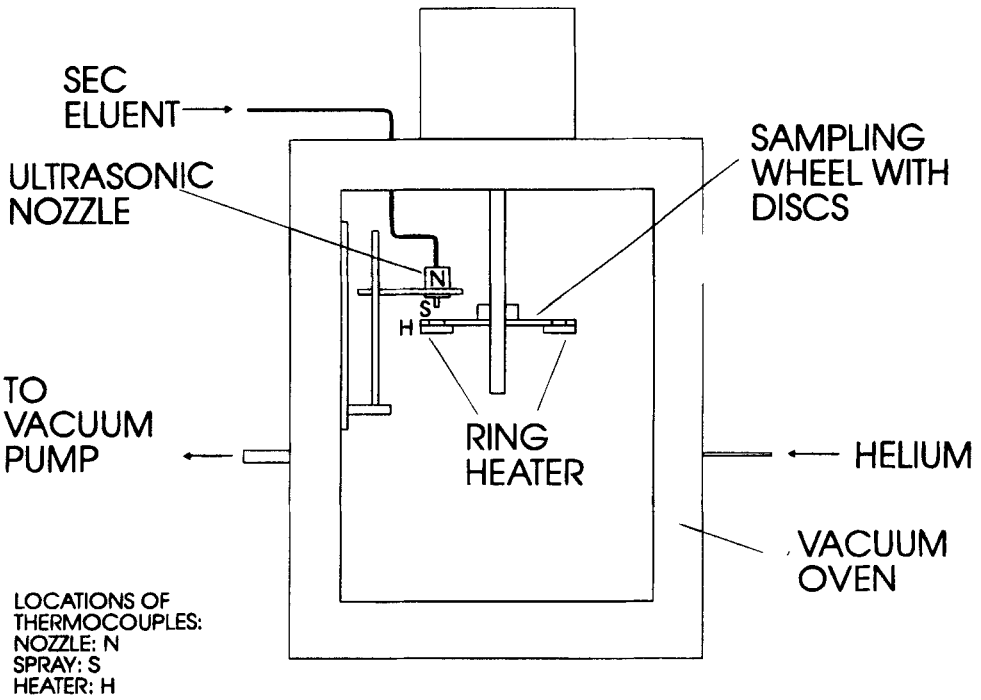

FIGURE 2 Schematic diagram of the solvent-evaporation interface (Interface I). The thermocouple locations are designated as: H close to the ring heater, *S* close to the polymer solution spray, and *N* inside the ultrasonic nozzle housing.

uid chromatograph (Norwalk, Connecticut) on a three-column set of PLgel 10-μm mixed-bed columns. The mobile phase was 1.0 mL/min freshly distilled tetrahydrofuran (THF). Samples were prepared as 0.17 wt % of each polymer in THF and injection volume was 200 μL. Polymer elution was monitored with a Waters model R401 DR.

The polymer sample fractions of experiments 5 through 8 were deposited with a solvent-evaporation interface similar in design to that of Dekmezian *et al.* [1] and denoted here as "Interface II." Polymer blend fractions of 20 s duration were spray deposited onto 110°C 13 × 2 mm germanium discs at 4.3 kPa in a 80°C chamber. Eluent spray was produced with a 120 kHz Sono-Tek ultrasonic nozzle driven at 3.0 W. The temperature of the interface vacuum chamber and sample collection platform were controlled separately by circulating silicone oil from Haake Inc. (Paramus, New Jersey) model DC5-GH and A81 baths, respectively.

Analytical Techniques Applied to Polymer Films

FTIR and Micro-FTIR. A Mattson Galaxy 6020 FTIR spectrometer (Madison, Wisconsin) and a Spectra-Tech IR-Plan FTIR microscope (Stamford, Connecticut) equipped with mercury-cadmium-telluride (MCT) detectors were used. All the FTIR spectra taken with the Mattson bench were averaged with 128 scans at 4 cm^{-1} resolution. The micro-IR spectra were averaged with 200 scans at the same resolution and were taken with an square aperture of about 30 × 30 μm. All the spectra shown in this study were not baseline corrected.

Optical Microscopy. A Nikon Labophot-2 optical microscope (Tokyo, Japan) equipped with a reflectance assembly and a digital camera were used.

Laser Confocal Fluorescence Microscopy. A Bio-Rad MRC-600 dual-channel confocal scanning laser microscope (Wadford, England) with a krypton-argon laser was used to investigate the morphology of samples of polymer blends, where one polymer was labeled with NBD. The microscope is a Nikon Optiphot with super-high-pressure mercury lamp. Data acquisition and image filtering was performed by an IBM PC with Bio-Rad software. The focal point for the laser was usually the center and surface of the film. The resulting fluorescent emission of the NBD is detected. The laser power was varied when the fluorescence signal was too weak or too strong to provide good contrast. The image was acquired and averaged using a Kalman filtering algorithm (Wadford, England).

Fluorescence Spectroscopy. The steady-state fluorescence energy transfer was measured. The donor and acceptor used were phenanthrene-labeled polystyrene and anthracene-labeled poly(methyl methacrylate), respectively. A SPEX Fluorolog 2 spectrometer (Edison, New Jersey) equipped with double-grating monochromators and a red-sensitive photomultiplier and photon-counting detection was used. The polymer blend samples on germanium discs were placed such that the light from the source illuminated the center of the disc. With the use of front-face geometry, 1-nm resolution and an integration time of 2 s, emission spectra at an excitation wavelength of 296 nm were obtained. The raw data were then divided by the reference intensity to correct for wavelength-dependent light intensity variations. From the corrected emission spectrum, two intensities were obtained: I_D at 366 nm, where it was assumed that the intensity was wholly due

to donor (Phe) fluorescence, and I_A at 411 nm, where it was assumed that the intensity was wholly due to acceptor (An) fluorescence. The basis for the above assumptions was that the intensities of An at 366 nm was negligible and Phe at 411 nm was small.

RESULTS AND DISCUSSIONS

Figure 3 shows a plot of temperatures measured inside Interface I during a typical SEC run. The curves represented the temperatures measured 1 mm from the disc heater (thermocouple H), 2 mm from the polymer solution spray (thermocouple S), and inside the ultrasonic nozzle (thermocouple N). The spray of polymer solution from SEC began at time equal to 1 min and ended at 24 min. The temperature profiles show that a steady state was reached within the first 5 min as measured by thermocouples. Thermocouple N varied only 2°C during the spray, but the vaporization of spray cooled the immediate surroundings of the heater by more than 15°C (thermocouple H) and the spray path by about 25°C (thermocouple S). Therefore, good conduction of heat towards the spray and discs was required to avoid accumulation of TCB in the interface and to ensure the system could reach steady state in a reasonable time.

Figures 4A, 4B, 4C and Figure 5 show results for one of the fractions collected from experiment 1 using NBD-labeled polyethylene. In this case, the collected fraction was

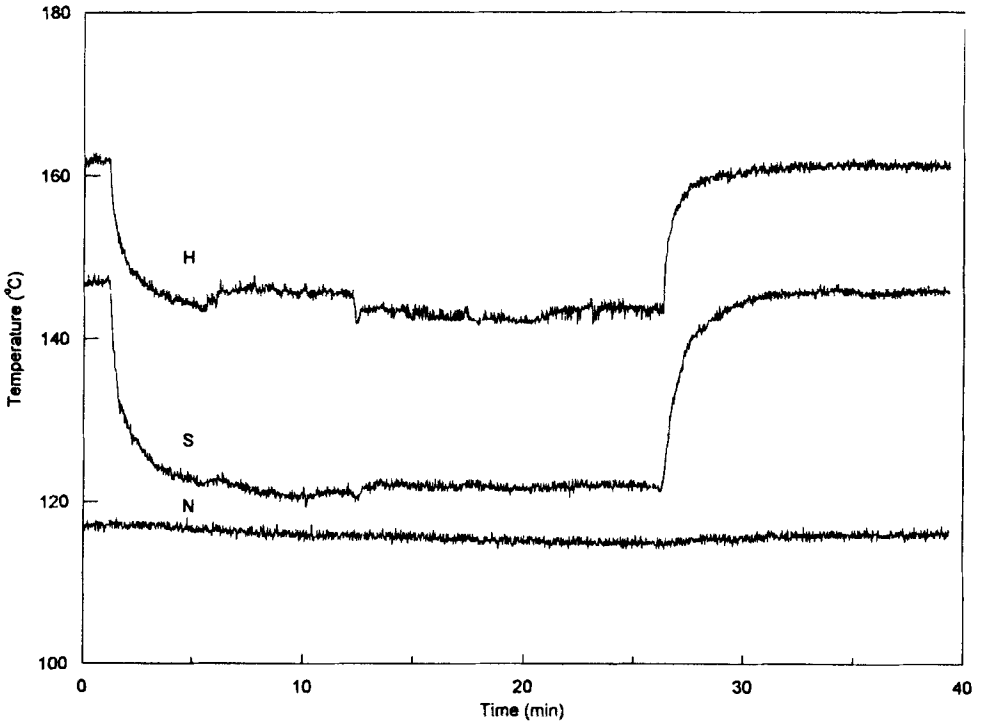

FIGURE 3 Temperatures measured by the thermocouples (H, S, and N) shown in Figure 2 during an SEC experiment with evaporation of 1,2,4-trichlorobenzene at a flow rate of 0.5 mL/min.

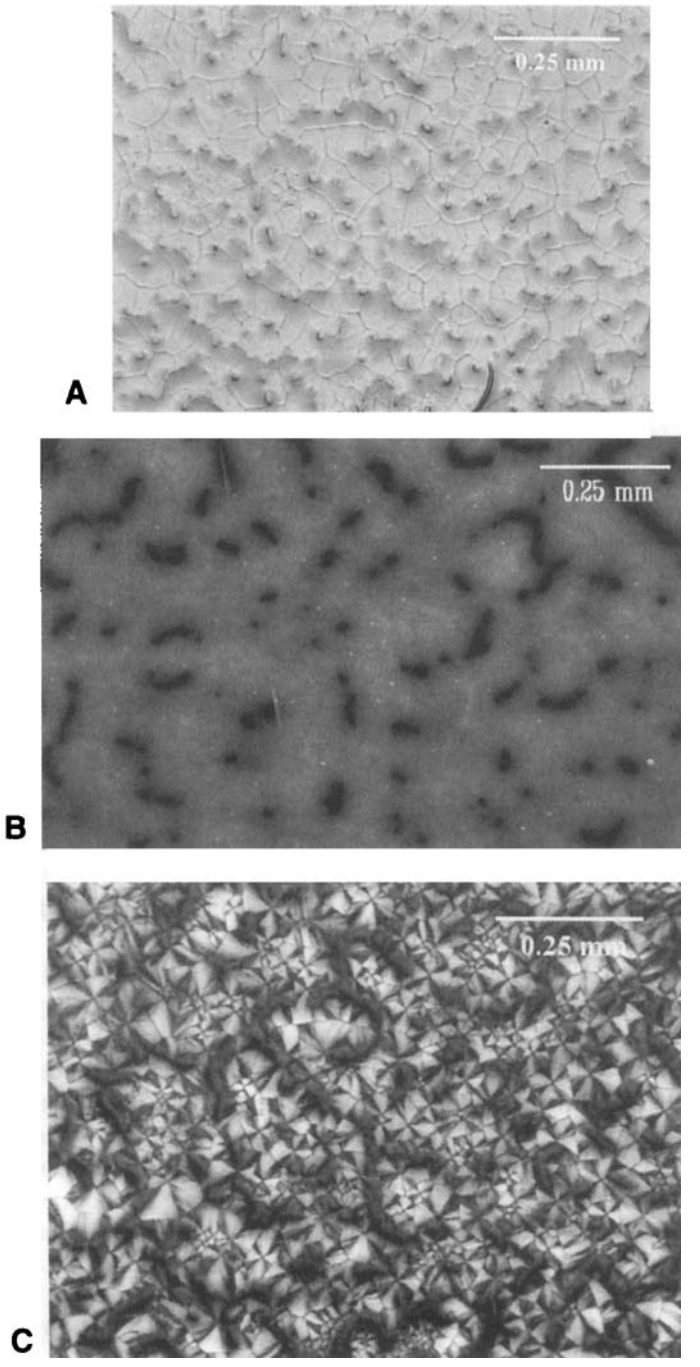

FIGURE 4 Microscopy photographs (A: optical, B: laser confocal fluorescence, and C: optical with crossed polarizers) of a 3.0 min SEC (0.3 mL/min) fraction of NBD-labeled polyethylene (experiment 1 of Table I) near the chromatogram maximum on a KCl substrate.

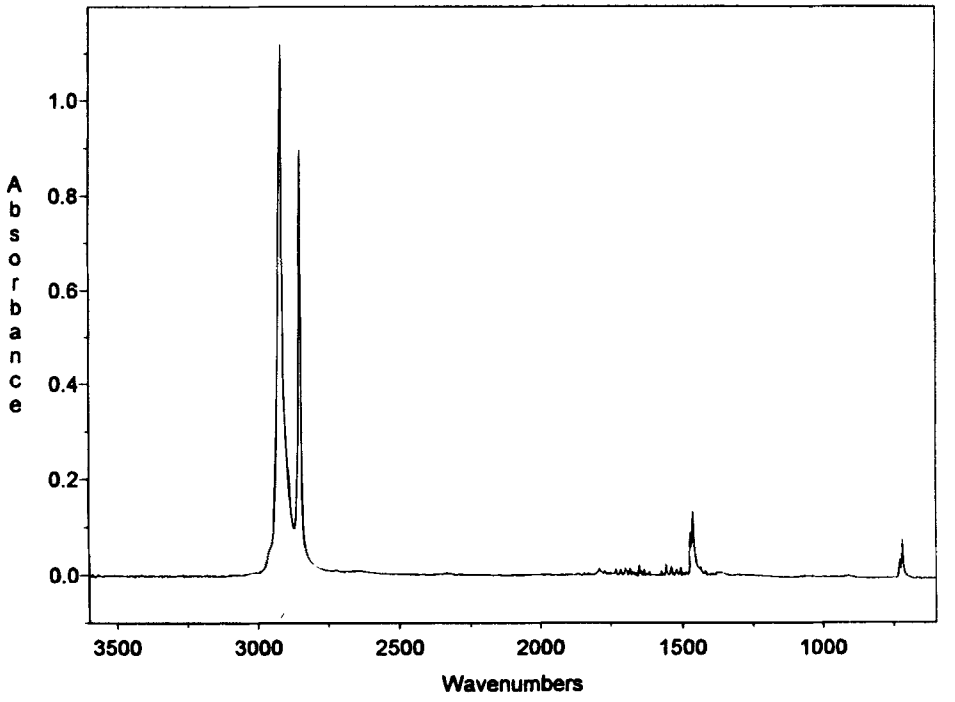

FIGURE 5 The corresponding FTIR spectrum of the polymer deposit shown in Figure 4.

close to the chromatogram maximum and was within a molecular weight range of 32,000 to 50,000 g/mol (using a linear low-density polyethylene calibration curve). The disc substrate was potassium chloride and this fraction was collected over a period of 3 min. All other results in this paper utilized germanium as the substrate. This included the duplicate SEC fractionation of experiment 1.

As shown in Figure 4, all microscopy results (A: optical, B: laser confocal fluorescence, C: optical with crossed polarizers) show the film to be irregular in that many holes where little or no polymer is present can be observed. However, these small holes did not affect (at least superficially) the FTIR spectrum, as shown in Figure 5 in which an excellent baseline was obtained. However, another concern here relevant to quantitative spectral interpretation is the effect of crystallinity on the spectrum. For polyethylene, the doublets at 1463 cm^{-1}/1473 cm^{-1} and 721 cm^{-1}/734 cm^{-1} are well known to be sensitive to crystallinity [12]. In our experiments, crystallinity could vary among fractions based on polymer molecular weight and deposition conditions. No further attempt was made to quantitatively interpret this spectrum. Instead, quantitative effects regarding the spectra of an amorphous polymer, polystyrene, will be discussed. In Figure 4C, polyethylene spherulites were observed throughout the polymer deposit. The bulky NBD groups along the polyethylene chains did not seem to inhibit crystallization.

The next fraction (not shown) collected in the same SEC run displayed a similar film but showed very low fluorescence by laser confocal fluorescence microscopy. FTIR spectra showed the film to be of similar thickness to other films which showed much stronger

fluorescence. The reason for this phenomena is not known at this point. It may be associated with how the labels are distributed with respect to molecular weight of the polyethylene. However, in another SEC run with fractions collected on germanium discs, the fluorescence intensity of each fraction appeared to be proportional to the amount of deposited polymer across the whole molecular weight range, as expected.

Figure 6 shows the FTIR spectrum for an SEC fraction of unlabeled polystyrene (experiment 2). The FTIR spectrum shows evidence of the baseline wandering. The inset of film morphology appears to show multiple irregular holes where little or no polymer is present. Table II shows the ratios of absorbances at different wavenumbers to the absorbance at 698 cm^{-1} for six different fractions from an SEC separation. The coefficient of variation (standard deviation/mean × 100%) of absorbance ratios ranged from 2 to 4% due to combined effects of light scattering and bare spaces on the films. Also shown on the table is the absorbance ratios of a cast polystyrene film. The ratios of the SEC fractions were about 10 to 22% higher than those of the cast film. This was attributed to the bare spaces in the film. Figure 7 shows the FTIR spectrum of a cast polystyrene film. The film was flat and continuous and the spectrum was excellent with no evidence of light scattering effects.

The optical photomicrograph in Figure 8A corresponds to an SEC fraction of NBD-labeled polyethylene and unlabeled polystyrene (experiment 3). The morphology consists of dispersed particles in a continuous matrix. The laser confocal fluorescence pho-

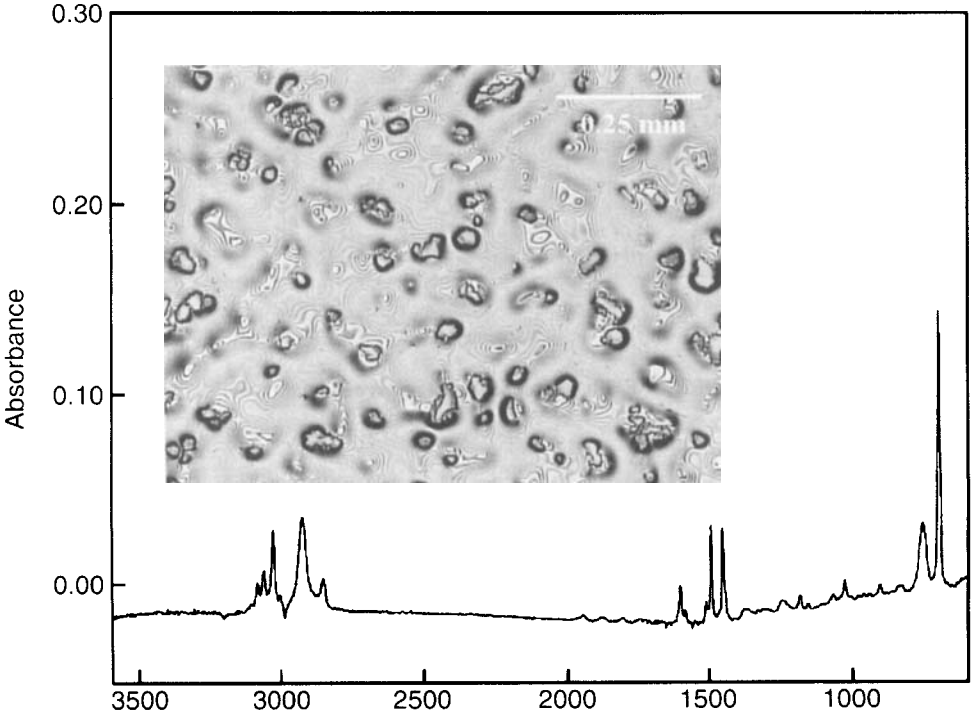

FIGURE 6 FTIR spectrum of an SEC fraction of unlabeled polystyrene (experiment 2 of Table I). The inset shows the optical photomicrograph of the film morphology.

TABLE II

Absorbance ratios of polystyrene films to 698 cm^{-1}.

Absorbance Ratio at Wavenumbers [cm–1]	Average Absorbance Ratio of Six Fractions	Standard Deviation of Average Absorbance Ratio	Absorbance Ratio of Cast Film
1452	0.333	0.012	0.289
1493	0.344	0.014	0.306
2924	0.336	0.007	0.276
3025	0.296	0.009	0.268

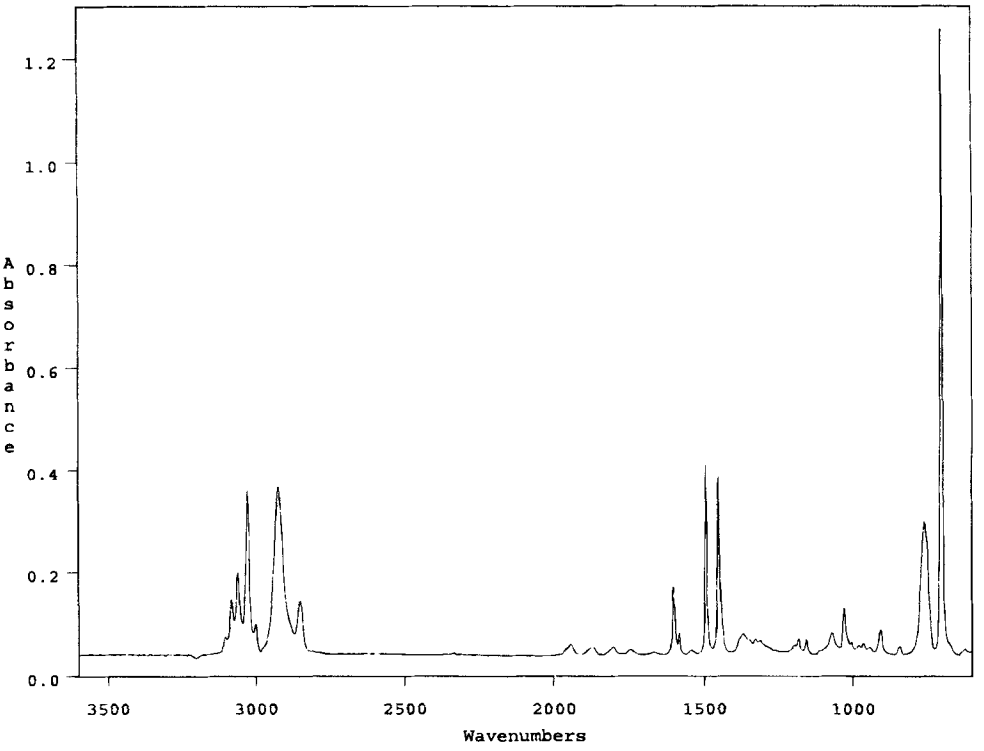

FIGURE 7 FTIR spectrum of a cast polystyrene film.

tomicrograph of the same fraction is shown in Figure 8B. The confocal image at first appeared to show NBD-labeled polyethylene dispersed in a polystyrene matrix. However, examination of the sample using both transmission and reflectance micro-FTIR spectroscopy revealed that the dispersed phase was composed of a mixture of polyethylene and polystyrene. Furthermore, the matrix was found to consist of only polyethylene (despite the fact that it was not fluorescing).

The transmission spectrum of infrared scans on a particle is shown in Figure 9A whereas that on the matrix immediately next to the particle is shown in Figure 9B. There were no absorption bands due to polystyrene ring C–H stretching between 3029 and 3138 cm^{-1} or ring skeleton in-plane bend or stretch at 1493 cm^{-1} and 1450 cm^{-1} [12] in both trans-

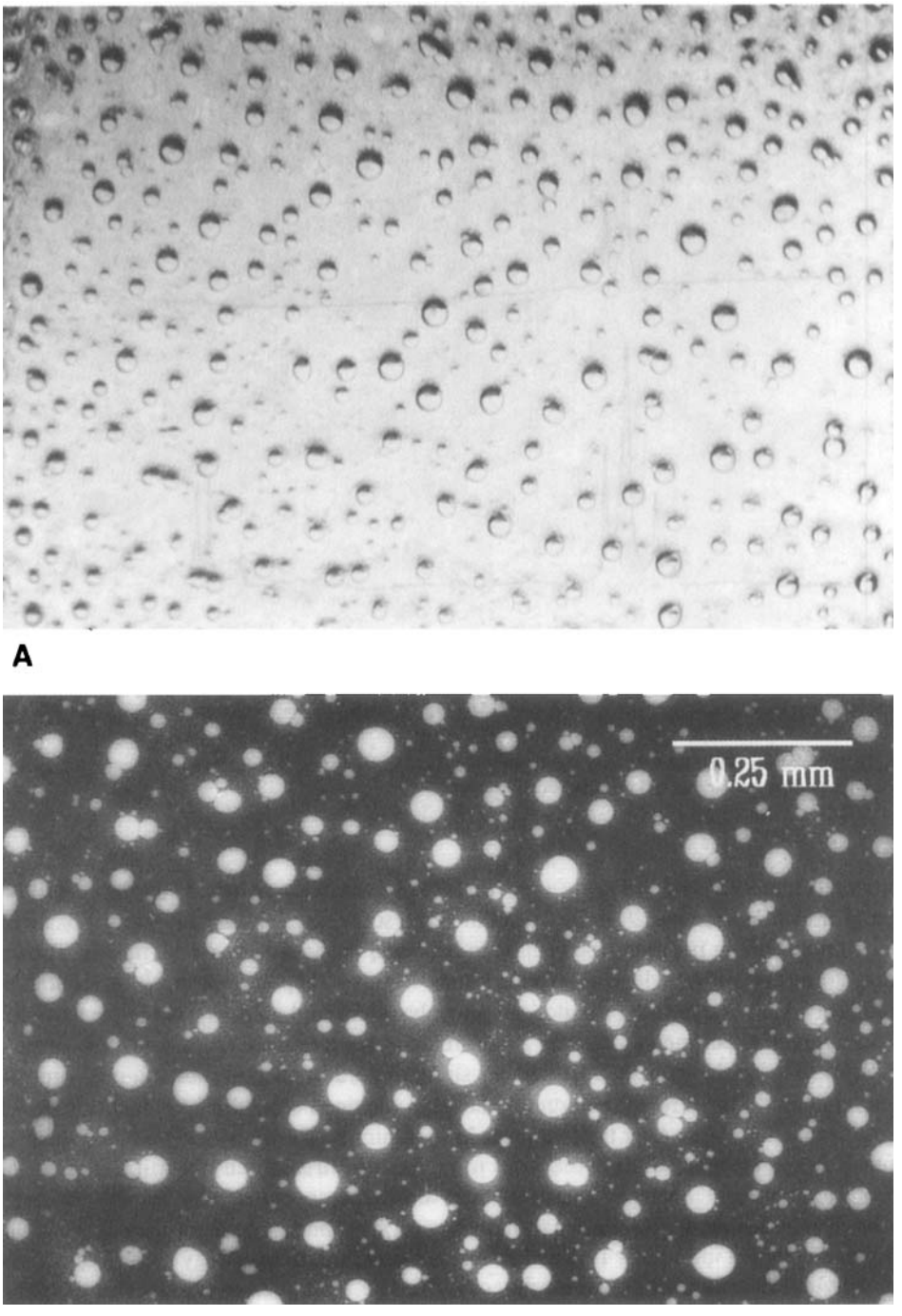

FIGURE 8 Optical (A) and laser confocal fluorescence (B) photomicrographs of an SEC fraction of NBD labeled polyethylene and unlabeled polystyrene blend (experiment 3 of Table I). The scale bar of 8B divided by 1.36 applies to 8A. (**See Color Plate I**).

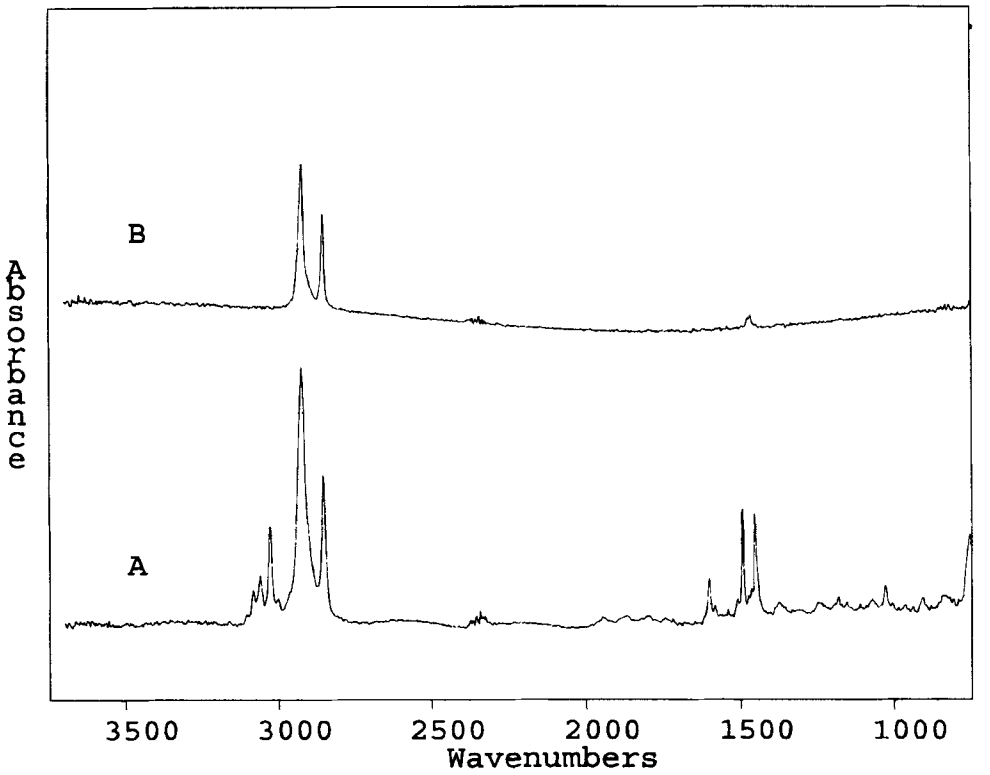

FIGURE 9 Micro-FTIR transmission spectra of domains of the polymer deposit shown in Figure 8. Spectrum of a dispersed phase particle (A) and continuous matrix (B).

mission (Figure 9B) and reflectance spectra (not shown) of the matrix. Only the absorption due to stretching (around 2900 cm^{-1}) and in-plane scissoring (around 1470 cm^{-1}) of methylene groups along polyethylene [12] were observed in the spectra of the matrix. Typical polystyrene and polyethylene absorption bands, however, appeared at those wavenumbers in Figure 9A, indicating the presence of both polystyrene and polyethylene in the particles.

Subsequent experiments involved a post-run solvent treatment using a respray of pure TCB for 90 s on the deposited film under similar operating conditions as a post-run solvent treatment. The infrared spectrum of the same fraction before the treatment was shown in spectrum A and that after the treatment in spectrum B of Figure 10. Even though spectrum B had a steeper baseline than spectrum A, the Christiansen distortion around the absorption bands at 700 cm^{-1} and 1500 cm^{-1} almost disappeared after the solvent treatment. The optical and laser confocal fluorescence photomicrographs of the solvent treated film are shown in Figures 11A and B, respectively. The morphology appeared to show polyethylene distributed more uniformly over the disc. One interpretation is that the polyethylene was transported over the surface by the dissolution of the polystyrene in the TCB. The solvent treatment improved the film uniformity and spectrum appearance, although some baseline slope was still apparent. The results were consistent with prior observations of solvent annealing effects [4].

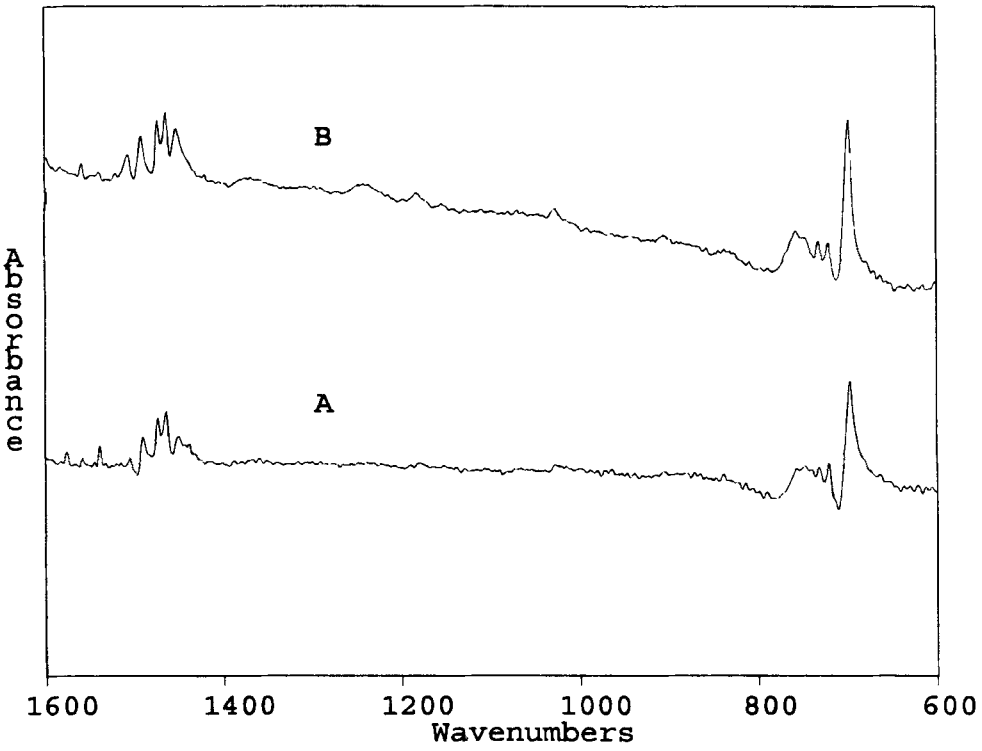

FIGURE 10 FTIR spectra before (A) and after (B) a 90-s post-run solvent treatment respray with pure TCB of the polymer deposit shown in Figures 8 and 9.

In another experiment, tetrahydrofuran (THF) was applied to the disc surface of a fraction collected in the duplicate run of experiment 3. Before the application of THF, the optical and laser confocal fluorescence photomicrographs of the fraction were similar to Figures 8A and B, respectively. As shown in Figure 12, all microscopy results (A: optical, B: laser confocal fluorescence, C and D: optical with crossed polarizers at different magnifications) show that the THF washed away the dispersed phase and left halos of fluorescent material in place of the dispersed phase. Furthermore, small spots of fluorescent, crystalline polymer were evident within some of the halos. The crystalline nature of these spots is clearly evident in the optical photomicrographs using crossed polarizers. Apparently, the NBD-labeled polyethylene was more compatible with the polystyrene because of the similarity in structure, causing it to be concentrated in and near the phase separated polystyrene domains. The remaining polyethylene formed a thin film with a low concentration of fluorophores. It is possible, that in this case, the primary reason that the polyethylene in the matrix is not fluorescing, except at the borders of the dispersed phase, is the film of the matrix is so thin that there is insufficient concentration of labels remaining to provide observable fluorescence.

NBD-labeled polyethylene and unlabeled polypropylene (experiment 4) provided reasonable FTIR spectra, but rather weak fluorescence (except for the occasional cluster of bright spots). The film appeared moderately rough with valleys representing spots uncoated by polymer.

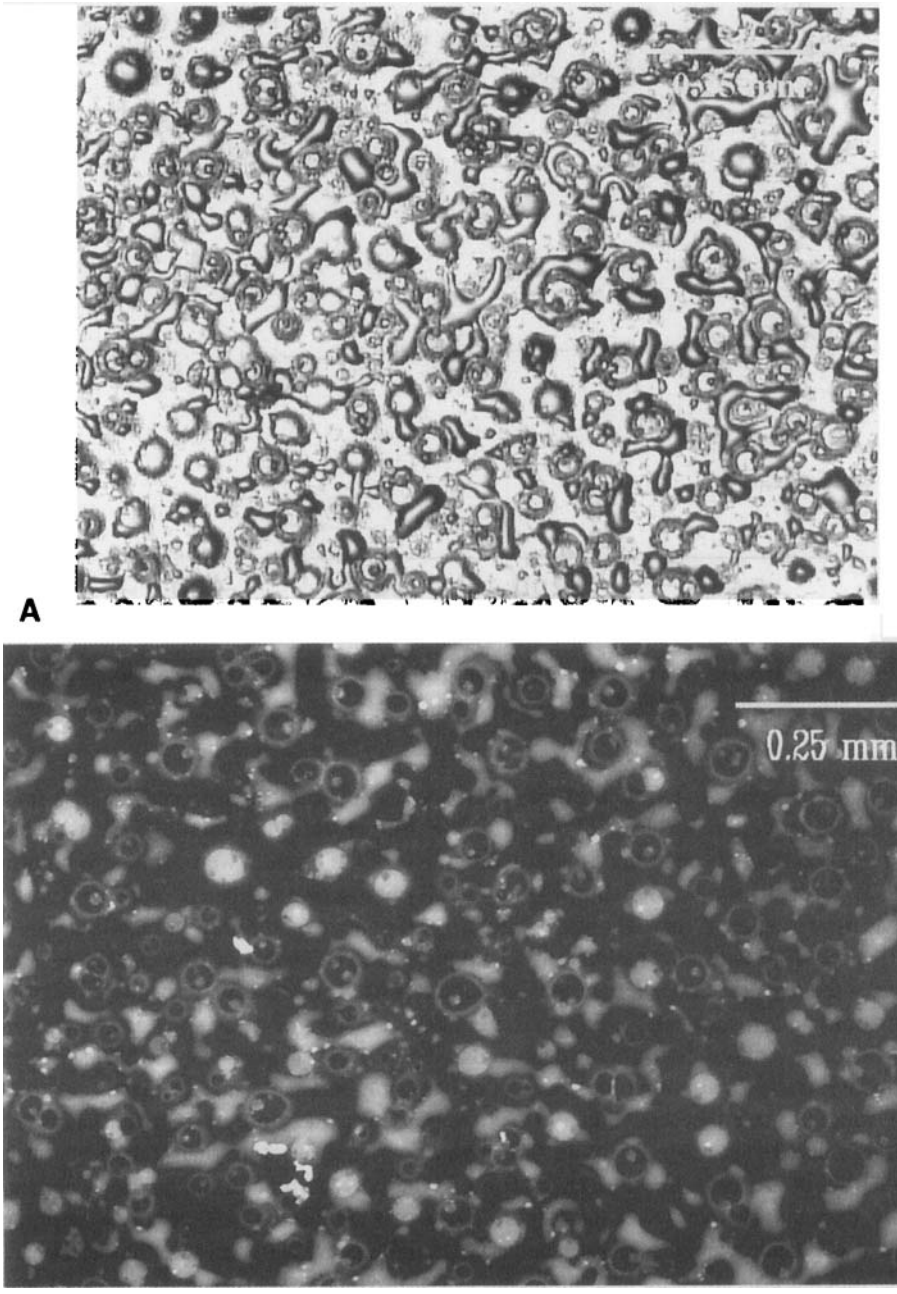

FIGURE 11 Optical (A) and laser confocal fluorescence (B) photomicrographs of the TCB respray-treated polymer deposit of Figure 10.

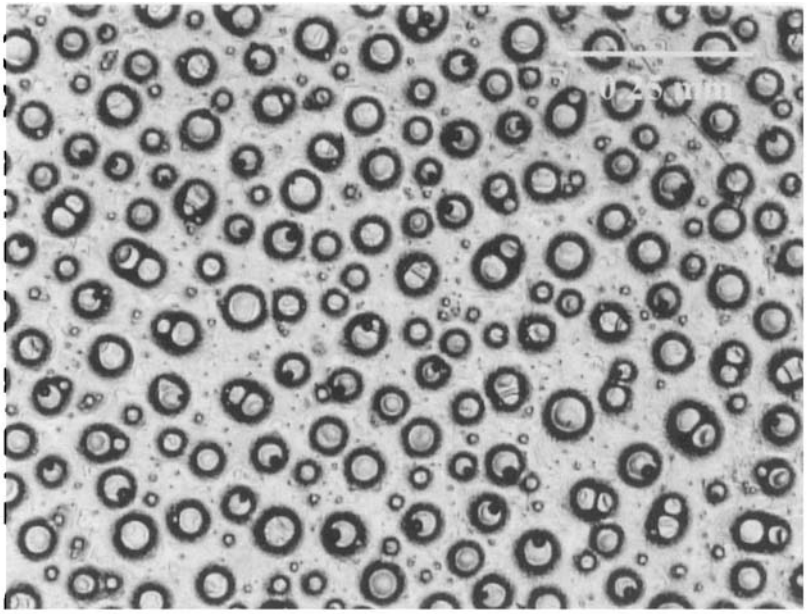

A

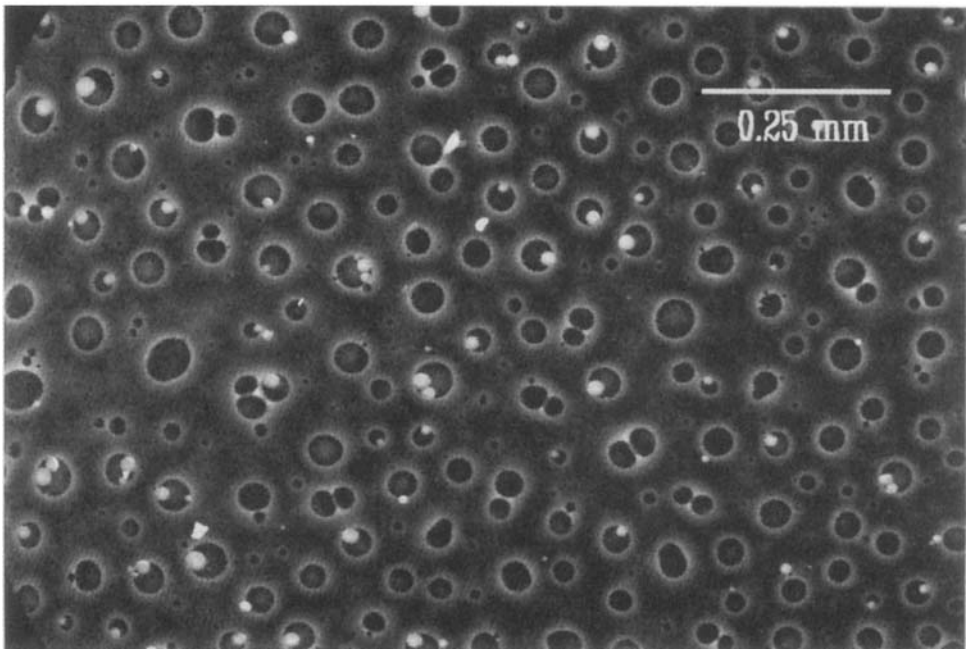

B

FIGURE 12 Microscopy photographs (A: optical, B: laser confocal fluorescence, C and D: optical with crossed polarizers at different magnifications) of a polymer deposit similar to that of Figure 8 after THF washing.

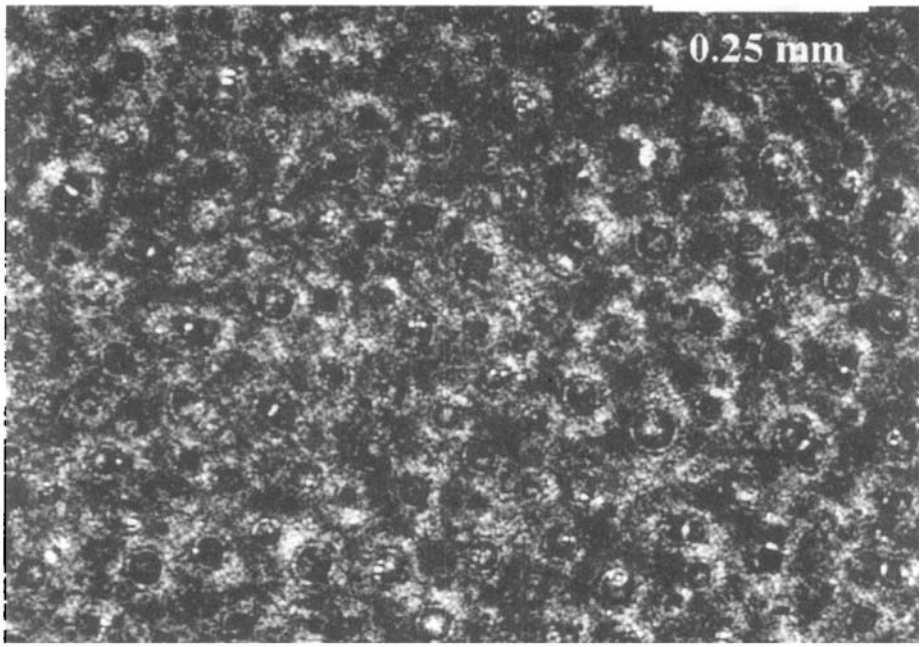

C

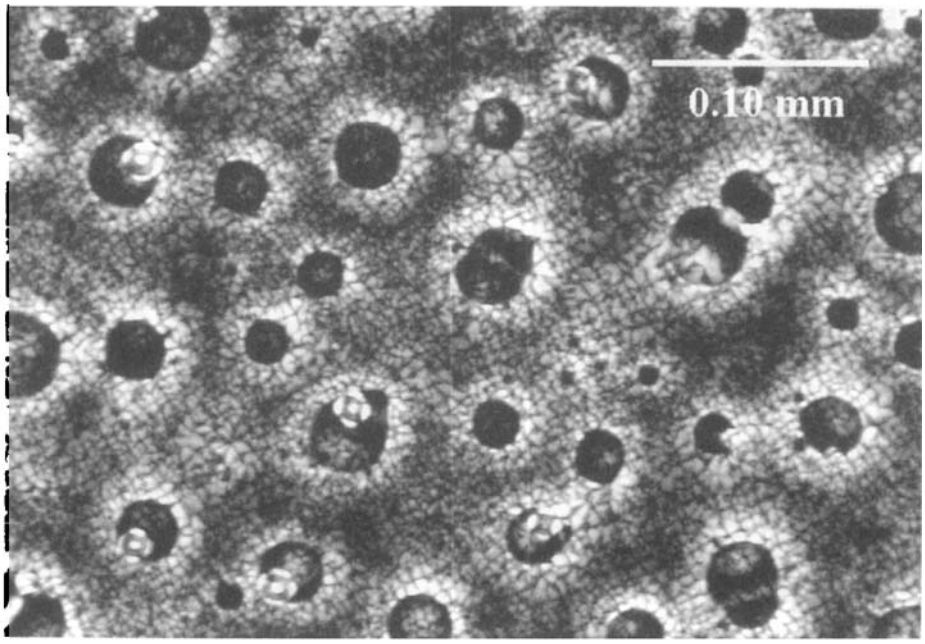

D

FIGURE 12 (*Continued*)

Blends of polystyrene and poly(methyl methacrylate) (experiment 5 to 7) showed films with no dispersed phase evident, probably due to the high intensity of fluorescence which had blocked out any visual observation of phase separation. The black holes observed in the photomicrographs are bare spots in the coating. FTIR spectra showed some baseline wandering as a result of light scattering effects. The less the amount of polymer on the discs, the more variation in the baseline was observed.

In order to further evaluate the extent of phase separation which may occur during solvent-evaporation deposition of polymer blend films, polymers labeled with functional groups which form a donor-acceptor pair were employed. The efficiency of energy transfer between a donor-acceptor pair such as anthracene and phenanthrene is determined by the proximity of the tags to one another. Phenanthrene-labeled polystyrene and anthracene-labeled poly(methyl methacrylate) (experiment 8) showed FTIR spectra with some variation in slope but no serious distortions. Some bare spots were evident in the deposited films.

No laser confocal fluorescence microscopy was possible for experiment 8 because neither anthracene nor phenanthrene absorbed light at 488 nm. However, they do represent a donor-acceptor pair and therefore fluorescence spectroscopy was used to examine energy transfer as a function of retention volume in SEC (i.e., as a function of molecular weight). Figure 13 shows a typical emission spectrum obtained by exciting the sample at 296 nm with intensity measured as counts per second (cps) plotted against wavelength. Table III

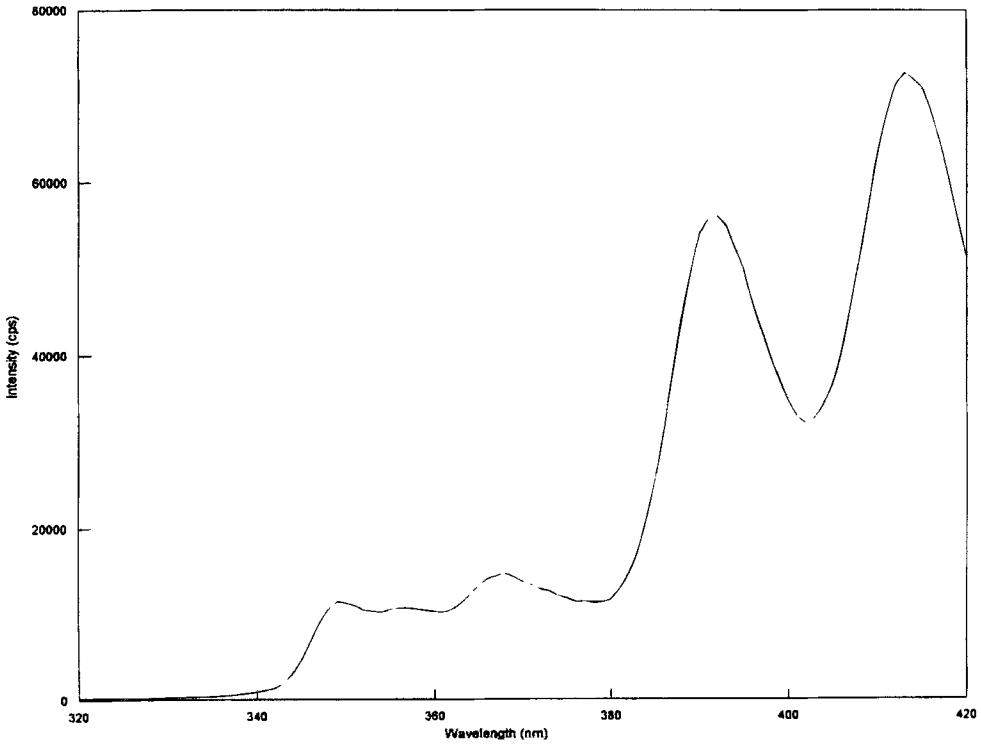

FIGURE 13 Emission spectrum of an SEC fraction from experiment 8 (Table I) obtained by exciting at 296 nm.

TABLE III

Emission intensity measurements of fractions collected in experiment 8.

Fraction Number	Emission at 366 nm (I_D) [cps]	Emission at 411 nm (I_A) [cps	I_D/I_A]
1	12400	3430	3.6
2	10000	13500	0.75
3	15200	23500	0.65
4	25100	66100	0.38
5	15000	40600	0.37
6	17200	47200	0.37

shows the ratio of the intensity at 366 nm (the donor) to that at 411 nm (the acceptor). The intensity values due to the donor and acceptor have been normalized to account for different compositions in each fraction. The fraction numbers were arranged in the order of decreasing molecular weight. The rapid decrease of this ratio with decreasing molecular weight shows the enhanced miscibility of the lower molecular weight compared to the higher molecular weight fractions. Moreover, this ratio appeared to level off rapidly at low molecular weight.

CONCLUSIONS

The combination of optical microscopy, laser confocal fluorescence microscopy, and FTIR spectroscopy showed that the film morphologies of polymer blends were sometimes quite complex and FTIR spectroscopy results could be readily affected by these morphologies. Sometimes distortions in FTIR spectra were obvious (Christiansen distortion or wavy baselines). However, at other times the primary effect was simply a change in the magnitude of an absorption band. These results demonstrate that, even for homopolymers, it is necessary to verify the accuracy of the spectra obtained from the solvent-evaporation interface samples by comparison with reference spectra obtained by more well-controlled methods (e.g., film pressing).

A major complication in defining the morphologies obtained was that the information provided by the laser confocal fluorescence microscope was difficult to interpret. In particular, some labeled polyethylene was found to show fluorescence while other portions did not. This behavior, which was only revealed by the application of combined analytical techniques, could be caused by nonuniform label concentration and distribution on the polyethylene. However, overall concentration of the label is known to be an order of magnitude greater than that usually used in fluorescence experiments with poly(methyl methacrylate)-polystyrene. It does point to the need to carefully characterize such labeled polymers and to critically examine confocal microscopy results.

Steady-state fluorescence spectra were used to obtain a measure of miscibility of polystyrene-poly(methyl methacrylate) blends as a function of molecular weight. This method is readily applied and potentially allows this type of information to be obtained. However, there was no attempt here to determine if polymer film morphology could also affect these fluorescence results.

Acknowledgements

We are very pleased to acknowledge that funding for this study was provided by the Eastman Kodak Company (Rochester, NY), the Ontario Center for Materials Research, and the Natural Sciences and Engineering Research Council of Canada.

References

1. A. H. Dekmezian, T. Morioka, and C. E. Camp, *J. Polym. Sci., Part B: Polym. Phys.*, **28**, 1903 (1990).
2. J. J. Gagel and K. Biemann, *Mikrochim. Acta.*, **11**, 185 (1988).
3. P. Cheung, S. T. Balke, T. C. Schunk, and T. H. Mourey, *J. Appl. Polym. Sci., Appl. Polym. Symp.*, **52**, 105 (1993).
4. T. C. Schunk, S. T. Balke, and P. Cheung, *J. Chromatogr. A.*, **661**, 227 (1994).
5. P. C. Cheung, S. T. Balke, and T. C. Schunk, In *Chromatographic Characterization of Polymers*; T. Provder, H. G. Barth, and M. W. Urban, Eds.; Advances in Chemistry 247; American Chemical Society: Washington, DC, 1995; p 265.
6. W. C. Price and K. S. Tetlow, *J. Chem. Phys.*, **16**, 1157 (1948).
7. N. Jones, *J. Amer. Chem. Soc.*, **74**, 2681 (1952).
8. R. H. Webb, *Opt. Photonics News*, **2(7/8)**, (1991).
9. P. B. Ghosh and M. W. Whitehouse, *Biochem. J.*, **108**, 155 (1968).
10. F. Amrani, J. M. Hung, and H. Morawetz, *Macromolecules*, **13**, 649 (1980).
11. S. Sosnowski, J. Feng, and M. A. Winnik, *J. Polym. Sci., Part A, Polym. Chem.*, **32**, 1497 (1994).
12. D. I. Bower and W. F. Maddams, *The Vibrational Spectroscopy of Polymers*; Cambridge University: New York, 1989, pp 162–200.